

---

# TOWARDS MORE HOLISTIC INTERPRETABILITY: A LIGHTWEIGHT DISENTANGLED CONCEPT BOTTLENECK MODEL

---

**Gaoxiang Huang**

Deep Interdisciplinary Intelligence Lab  
HKUST(GZ)  
Guangzhou, China  
ghuang991@connect.hkust-gz.edu.cn

**Songning Lai, Yutao Yue \***

Deep Interdisciplinary Intelligence Lab  
HKUST(GZ)  
Guangzhou, China  
{songninglai, yutaooyue}@hkust-gz.edu.cn

## ABSTRACT

Concept Bottleneck Models (CBMs) enhance interpretability by predicting human-understandable concepts as intermediate representations. However, existing CBMs often suffer from input-to-concept mapping bias and limited controllability, which restricts their practical value, directly damage the responsibility of strategy from concept-based methods. We propose a lightweight Disentangled Concept Bottleneck Model (LDCBM) that automatically groups visual features into semantically meaningful components without region annotation. By introducing a filter grouping loss and joint concept supervision, our method improves the alignment between visual patterns and concepts, enabling more transparent and robust decision-making. Notably, Experiments on three diverse datasets demonstrate that LDCBM achieves higher concept and class accuracy, outperforming previous CBMs in both interpretability and classification performance. By grounding concepts in visual evidence, our method overcomes a fundamental limitation of prior models and enhances the reliability of interpretable AI.

**Keywords** Concept-based Models, Disentanglement, Explanable AI

## 1 Introduction

Deep learning has achieved unprecedented success in fields such as image recognition and natural language processing, driving the rapid development of AI and transforming our lives. However, its inherent "black-box" nature makes the decision-making process difficult to explain and understand. Especially in critical applications (e.g., healthcare, law, autonomous driving), we not only need high performance but also interpretability and trustworthiness. To address the "black-box" problem, explainable AI (XAI) has emerged[1]. It aims to reveal the internal mechanisms of models, enabling both experts and ordinary users to understand why AI makes a particular decision. Among numerous XAI methods like Prototypical Networks[2], Spare Autoencoder[3] etc, where Concept Bottleneck Models (CBMs)[4] have attracted significant attention due to their unique "conceptualized" intermediate layers regardless of computer visual and natural language process[5] tasks. CBMs first identify human-understandable "concepts" (e.g., presence of a beard, wearing glasses) and then make final predictions (e.g., identifying a person's identity) based on these concepts. This two-stage structure inherently provides interpretability, making CBMs well-suited for interpreting the relationship between an input image and its output class predictions via intermediate, human-understandable concepts.

Despite recent work that has narrowed the performance gap between CBMs and black-box models[6, 7, 8, 9], the interpretability of existing CBMs primarily stems from the transparency of the concept-to-label prediction. Fewer works have focused on solving the problem of input-to-concept mapping, which remains opaque and uncontrollable for human understanding. As shown in Figure 1, many concept predictions are frequently mislocalized in images. For instance, a bird's most important attributes (e.g., body, head, tail, bill) are often misidentified in the background or other irrelevant regions. Furthermore, the attribute mapping can be biased across different regions; for example, a "body" attribute may be reflected in visual patterns associated with the head and tail, even though they are visually

---

\*Corresponding author: Prof. Yutao Yue

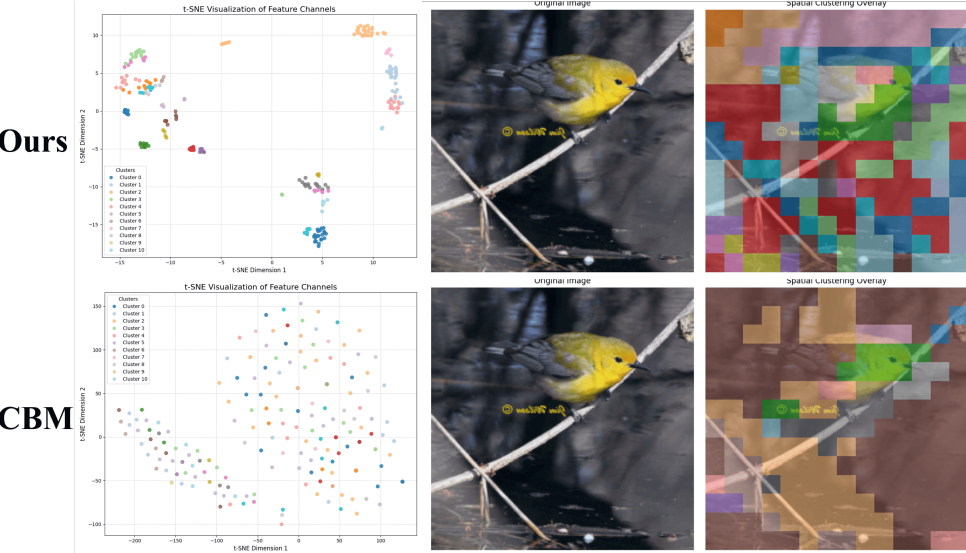


Figure 1: Case Study: Our proposed LDCBM and vanilla CBM, those t-SNE visualizations of visual pattern cluster relationship learnt in CUB dataset. The different colors in the t-SNE plots and spatial overlays represent distinct feature clusters.

unconnected. This leads to classifications based on spurious correlations[10, 11] and introduces data bias[12, 13] that compromises subsequent interpretability strategies. To fill this gap, some recent studies have attempted to improve input-to-concept interpretability through learnable prototypes and an untrustworthiness score alignment to approximate visual patterns and concepts [14, 15]. However, this approach lacks steerability, prototype is hard to align concept automatically Furthermore, DOT-CBMs[16] disentangle and extract a priority image patch to align with concept ground truth. Yet, these crops depend excessively on regular patches and cannot express the complete concept feature. Besides, Prototype-based method[17] was considered to align with concept, but merely calculate the similarity with concept to show the performance without the optimal target between both of prototype and concept. These methods either have great disentanglement of visual pattern to approach concept ground-truth and need great deal of human cost, or have directly gradient-based method between visual-pattern and concepts that leave the performance-interpretability trade-off.

In response to these limitations, we draw inspiration from the ICCNN[18, 19] and Prototypical Networks[20, 21] framework and its focus on feature map-based analysis. We propose LDCBM to provide improved interpretability on the mutual visual region-concept relationship. Specifically, we introduce an lightweight optimizable disentanglement of image components to automatically adjust the semantic composition, rather than prior cropping images into a grid. This is achieved by using an auxiliary loss to group similar-sized feature maps in the backbone and separate different groups.

To sum up, the key contributions of this work are as follows:

- We systematically analyze the key gap in visual-to-concept mapping and propose a method to improve it and can apply in some of precious CBM achieving better performance.
- We introduce LDCBM that automatically disentangles the key components of the input by leveraging feature maps for more interpretable and clear concept prediction.
- Experimental results demonstrate that our model surpasses other improved CBMs and achieves higher performance on three datasets, covering a range from coarse to fine-grained and small to large scale.

## 2 Methodology

### 2.1 Preliminary

**Concept Bottleneck Models:** Black-box models with bottleneck on human-annotation concepts, which first predicts the concepts, then uses the predicted concepts to make a final prediction. A Concept Bottleneck Model (CBM) consists of two predictors: a *concept predictor* and a *class predictor*. Given a labeled dataset  $\mathcal{D} = \{(x^{(n)}, c^{(n)}, y^{(n)})\}_{n=1}^N$ , where

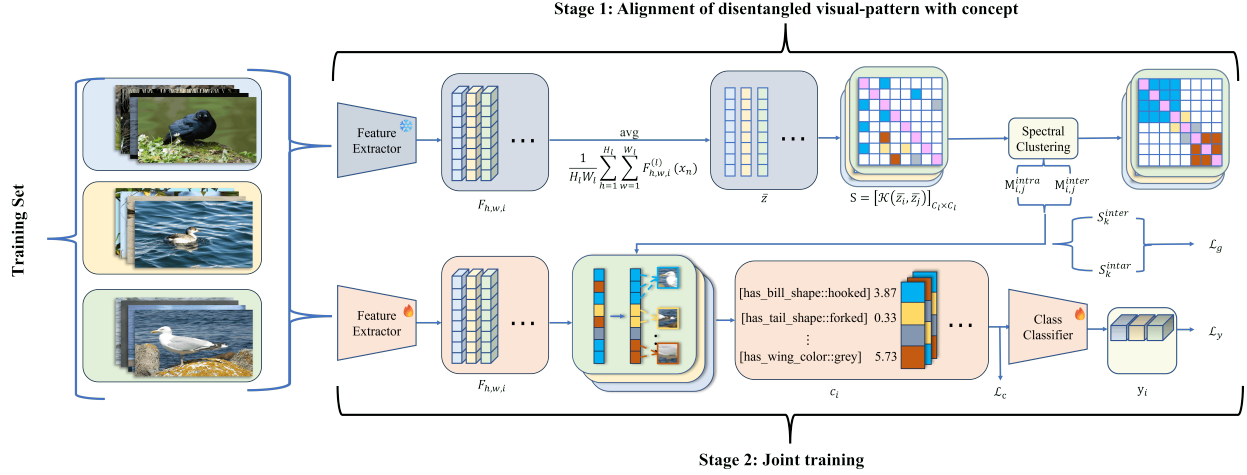


Figure 2: Overview of our LDCBM. It includes two stages modules: Alignment of disentangled visual-pattern with concept and Joint training among concept and class. The first forwards to get feature map and cluster for the intra and inter group mask what conduct the filter to concern specific visual pattern. The second do joint train from input to concept, and then mapping the concept to final task classification

the input  $x^{(n)} \in \mathcal{X}$ , the target  $y^{(n)} \in \mathcal{Y}$ , and the human-annotated concepts  $c^{(n)} \in \mathcal{C}$ , in this supervised concept-based model setting, the additional annotated concept vectors  $c^{(n)} \in \{0, 1\}^M$ ,  $M$  is the dimension of a concept. For a given input  $x$ , the concept predictor maps it to the concept space  $C$ , denoted as  $g_{X \rightarrow C}$ . Then, the output of the first model, the concepts  $c$ , is taken as the sole input and mapped to the label  $y$ , denoted as  $f_{C \rightarrow Y}$ . Thus, the training process of CBMs is supervised to encourage the alignment of  $\hat{c} = g(x)$  and  $\hat{y} = f(g(x))$  with the true concept and class labels, respectively.

**Compositional Models:** In order to automatically learning the compositional features[22] without the human-annotation in images region to play a compositional representation separator. We have the following loss to learn filter[18]:

$$\mathcal{L}_g(\theta, A) = - \sum_{k=1}^K \frac{S_{intra}^k}{S_k^{inter}} = - \sum_{k=1}^K \frac{\sum_{i,j \in A_k} s_{ij}}{\sum_{i \in A_k, j \in \Omega} s_{ij}}, \quad (1)$$

where  $s_{ij}$  is the similarity of sample  $i$  and  $j$  while  $i, j \in \{1, 2, \dots, n\}$ ,  $A = \{A_1, A_2, \dots, A_K\}$  split from the set of filter  $\Omega = A_1 \cup A_2 \cup \dots \cup A_K$ , where  $A_k$  is set of group  $k$  and  $A_i \cap A_j = \emptyset$ , Hence,  $S_{intra_k} = \sum_{i,j \in A_k} s_{ij}$  calculate the total similarity of all filter pair-wise in  $k$  group.  $S_{inter_k} = \sum_{i \in A_k, j \in \Omega} s_{ij}$  calculate the total similarity between filter in group  $k$  and all of filter except ground  $k$  in same layer.

This method aim to improve the relationship in same group, that filters in a same group will learn the similar visual pattern. and minimize relationship between different groups, that filters in different groups are able to learn segmentable visual pattern.

## 2.2 Lightweight Disentangled Concept Bottleneck Models

As shown in Figure 2, ours proposed LDCBM is conducted in two primary stages training: first, mapping the input image to a set of intermediate concepts, and second, mapping these concepts to the final class labels. The model is optimized by minimizing a total loss function,  $\mathcal{L}_{total}$ , defined as a weighted sum of three distinct components and is encouraged to minimize for LDCBM training:

$$\mathcal{L}_{total} = \mathcal{L}_y(f(c), y) + \lambda_c \mathcal{L}_c(g(x), c) + \lambda_g \mathcal{L}_g(\theta, A). \quad (2)$$

Here,  $\mathcal{L}_y$  represents the task loss for the final class prediction, which evaluates the output of the concept-to-label function  $f(c)$ .  $\mathcal{L}_c$  is the concept supervision loss for the middle concept prediction, applied to the output of the input-to-concept function  $g(x)$ . Finally,  $\mathcal{L}_g$  is a regularization term designed to encourage the disentanglement of learned features by structuring the parameters  $\theta$  of the feature extractor. The hyperparameters  $\lambda_c$  and  $\lambda_g$  control the relative influence of the concept supervision and feature disentanglement objectives, respectively.

### 2.2.1 Learning Disentangled Visual Features

To achieve feature disentanglement, we first process an input image  $x_n$  through the initial layers of our network. Let  $F^{(l)}(x_n) \in \mathbb{R}^{H_l \times W_l \times C_l}$  denote the feature map produced by the  $l$ -th layer, where  $H_l$ ,  $W_l$ , and  $C_l$  are the height, width, and number of channels[23], respectively. For each filter  $i \in \{1, \dots, C_l\}$ , we compute its global average response over the spatial dimensions  $(h, w)$  for a given input  $x_n$ :

$$\bar{z}_i(x_n) = \frac{1}{H_l W_l} \sum_{h=1}^{H_l} \sum_{w=1}^{W_l} F_{h,w,i}^{(l)}(x_n), \quad (3)$$

this value,  $\bar{z}_i(x_n)$ , represents the overall activation of filter  $i$  for the image  $x_n$ . To measure the functional similarity between any two filters,  $i$  and  $j$ , we define a similarity metric,  $s_{ij}^{(l)}$ , based on the correlation of their global average responses across a batch of  $N$  images. This metric is implemented as a kernel function  $\mathcal{K}(\cdot, \cdot)$ :

$$\begin{aligned} s_{ij}^{(l)} &= \mathcal{K}(\bar{z}_i, \bar{z}_j) \\ &= \rho_{ij}^{(l)} + 1 \\ &= \frac{\frac{1}{N} \sum_{n=1}^N (\bar{z}_i(x_n) - \mu_i)(\bar{z}_j(x_n) - \mu_j)}{\sigma_i \sigma_j} + 1. \end{aligned} \quad (4)$$

Here,  $\rho_{ij}^{(l)} \in [-1, 1]$  is the Pearson correlation coefficient[24] between the activation vectors of filters  $i$  and  $j$  over the batch. We shift the coefficient by +1 to ensure the similarity score  $s_{ij}^{(l)}$  is non-negative, ranging from 0 (perfectly anti-correlated) to 2 (perfectly correlated). The terms  $\mu_i = \frac{1}{N} \sum_{n=1}^N \bar{z}_i(x_n)$  and  $\sigma_i^2 = \frac{1}{N} \sum_{n=1}^N (\bar{z}_i(x_n) - \mu_i)^2$  represent the mean and variance of the global average response for filter  $i$  across the batch.

After getting the similarity, we need to certain the group decision cutting-edge. This step follows [18] using spectral cluster[25] to optimize the set of group  $A$  from set of all filter  $\Omega$  in Equation 1 Based on these group assignments, we construct an intra-group mask  $M^{intra}$  and an inter-group mask  $M^{inter}$ . The masks are defined by the indicator function  $\mathbb{I}(\cdot)$ , such that  $M_{i,j}^{intra} = \mathbb{I}(z_i = z_j)$  for filters  $i, j$  in the same group, and  $M_{i,j}^{inter} = \mathbb{I}(z_i \neq z_j)$  for filters in different groups. Hence,we can easily calculate the inter and intra group similarity is as follow:

$$\begin{aligned} -S_k^{intra} &= -\frac{1}{|M^{intra}|} \sum_{i,j} M_{i,j}^{intra} s_{ij}, \\ S_k^{inter} &= \frac{1}{|M^{inter}|} \sum_{i,j} M_{i,j}^{inter} s_{ij}. \end{aligned} \quad (5)$$

This allows us to formulate the disentanglement loss, which simultaneously maximizes the average similarity for filter pairs within the same group while minimizing the average similarity for pairs across different groups. This encourages filters within a group to learn functionally similar and cohesive representations.

Finally this similarity matrix, containing all  $s_{ij}$  values with certain group separation, is then used to compute the intra-group and inter-group similarity scores that form the disentanglement loss term,  $\mathcal{L}_g$ , as defined in Equation 1.

### 2.2.2 Concept Supervision

The disentanglement loss,  $\mathcal{L}_g$ , encourages filters to form semantically coherent groups by minimizing intra-group similarity and maximizing inter-group dissimilarity. This process establishes a latent association between visual patterns in the input image and specific filter groups. Building upon this structure, we introduce concept supervision to explicitly align these filter groups with human-understandable concepts.

Given a set of  $K$  filter groups, where each group  $A_k \in \mathcal{G}_i$ ,  $i \in \{1, \dots, M\}$  corresponds to a specific concept  $c_i$ , we aggregate the feature activations  $z_{\mathcal{G}_i}$  from the filters within that group. A concept classifier,  $g_c$ , which can be implemented as a simple linear layer, then maps these activations to a concept prediction. The concept supervision loss,

$\mathcal{L}_c$ , for a single concept is formulated using the Binary Cross-Entropy (BCE) as follows:

$$\begin{aligned}\mathcal{L}_c &= \sum_i \text{BCE}(g_c(z_{\mathcal{G}_i}), c_i) \\ &= \sum_i \text{BCE}(w_i \cdot z_{\mathcal{G}_i} + b_i, c_i),\end{aligned}\tag{6}$$

where  $w_i$  and  $b_i$  are the learnable weights and bias for the  $i$ -th concept classifier. This loss ensures that the filters in group  $\mathcal{G}_i$ , already predisposed to activating on similar patterns due to  $\mathcal{L}_g$ , are jointly optimized to detect the presence of concept  $c_i$ . Consequently, the total objective for the first training stage, mapping inputs to concepts ( $X \rightarrow C$ ), is the combined minimization of  $\mathcal{L}_g$ .

### 2.2.3 Concept-to-Class Prediction

The second stage of our framework learns the mapping from the intermediate concept representations to the final class predictions. This is achieved by taking the vector of predicted concept activations,  $c = [c^{(1)}, c^{(2)}, \dots, c^{(N)}]$ , from the bottleneck layer and feeding it into a final linear classifier to produce the class logits,  $\hat{y}$ . Following the standard CBM architecture, this relationship is defined as:

$$\hat{y} = W_y \cdot c + b_y,\tag{7}$$

where  $W_y$  is the weight matrix and  $b_y$  is the bias vector of the final classification layer. The objective for this second stage ( $C \rightarrow Y$ ) is the standard cross-entropy(CE) classification loss,  $\mathcal{L}_y$ :

$$\mathcal{L}_y = \text{CE}(\hat{y}, y),\tag{8}$$

where  $y$  is the ground-truth class label. Finally, the entire model is trained end-to-end by optimizing the total loss,  $\mathcal{L}_{\text{total}}$ , as defined in Equation 2, which integrates the objectives from both training stages.

## 3 Experiments

### 3.1 Experimental Setup

**Datasets:** We evaluate different methods on three real-world datasets, which vary in granularity and scale.

- **Caltech-UCSD Birds-200-2011 (CUB)**[26] is a fine-grained dataset containing 11,788 images. It includes 312 human-annotated attributes. Following the data processing in [4], we use a subset of 112 attributes from 15 parts of the birds as our concepts.
- **Large-scale CelebFaces Attributes (CelebA)**[27] is a large-scale human-face dataset with over 200,000 images across 10,177 classes. Each image is annotated with 40 face attributes, which serve as our concepts.
- **Animals with Attributes 2 (AwA2)**[28] is a coarse-grained dataset containing 37,322 images and 50 animal classes. Each image is annotated with 85 attributes, which are used as concepts.

**Baselines.** We compare our proposed LDCBM with two established baselines: Vanilla CBM [4] and Concept Embedding Model (CEM) [6]. The concept labels and data-processing methods are adopted from the original CBM and ECBM [7] papers. For our proposed benchmark, we train the models for 200 epochs, with the exception of the LDCBM, which is trained for 400 epochs (performing a spectral cluster every 2 epochs) to ensure the same number of gradient updates. Then, aim to suit the dataset, we have access to the annotation strategies, choose the number of cluster 16, 32, 32 for datasets CUB, CelebA and AwA2 respectively.

We use two metrics to evaluate the model’s performance: Concept Accuracy ( $C_{acc}$ ), which evaluates the model’s predictions for each concept individually, and Class Accuracy ( $A_{acc}$ ), which evaluates the overall classification task. The equations for these metrics are as follows:

$$C_{acc} = \frac{\sum_{n=1}^N \sum_{i=1}^M \mathbb{1}(c_i^{(n)} = \hat{c}_i^{(n)})}{N},\tag{9}$$

$$A_{acc} = \frac{\sum_{n=1}^N \mathbb{1}(y^{(n)} = \hat{y}^{(n)})}{N}.\tag{10}$$

Table 1: Generality Results: including the Concept accuracy and Class accuracy in three datasets(CUB, CelebA, AwA2) by four models. Bold indicates the best interpretable result, underline indicates the 2nd-best result.

Model	Data	CUB		CelebA		AWA2	
		Concept	Class	Concept	Class	Concept	Class
CBM		0.9220	0.6080	0.9121	0.5115	0.9355	0.7663
CEM		<u>0.9350</u>	0.6572	<u>0.9126</u>	0.5324	0.9366	0.7708
Ours		0.9291	<u>0.6617</u>	0.9115	<u>0.5324</u>	<u>0.9400</u>	<u>0.7755</u>
CEM+Ours		<b>0.9386</b>	<b>0.6636</b>	<b>0.9176</b>	<b>0.6350</b>	<b>0.9430</b>	<b>0.7841</b>

## 4 Result

### 4.1 LDCBM enhance the performance of both concept and class accuracy

Table 1 presents a comparative analysis of different models’ performance, specifically focusing on Concept and Class accuracy metrics across various datasets. All three evaluated models consistently achieve high concept accuracies, exceeding 90.0% with only marginal differences among them. However, LDCBM demonstrates a notable advantage in Class accuracy, particularly in challenging scenarios. On the large-scale CelebA dataset, LDCBM achieves the highest Class accuracy, matching CEM’s performance and surpassing CBM. Furthermore, in fine-grained tasks, such as those represented by the CUB dataset, LDCBM exhibits strong Class accuracy, closely approaching the top-performing CEM model and significantly outperforming CBM, while also maintaining a high concept accuracy. To further investigate the properties of LDCBM, we also evaluated The hybrid CEM+LDCBM model outperformed all three standalone models across all datasets. Notably, on the CelebA dataset, it achieved a class accuracy of 63.50%, surpassing CEM alone by approximately 10.26%. This substantial gain suggests that the disentanglement module from LDCBM enables the network to utilize concept information more effectively for classification.

This robust performance in Class accuracy, especially in fine-grained contexts, suggests that LDCBM effectively captures the pure and distinct features of concepts. These features are then robustly transferred to the interpretable decision-making process, ensuring that each concept functions as a unique and cognitively distinct component. This inherent capability not only enhances interpretability but also directly contributes to LDCBM’s superior Class accuracy compared to other methods.

### 4.2 LDCBM achieve the better efficiency trade-off Under Intervention

Concept interventions aim to evaluate a model’s reliance on its learned concepts by systematically correcting erroneous concept predictions or incorrecting right concept predictions to observe the impact on final class accuracy. As depicted in Figure 3, we progressively intervene four models vanilla CBM, CEM, LDCBM and hybrid model CEM+LDCBM on two dataset including fine-grained and coarse-grained that concern to test the effect of intervened concepts well.

The vanilla CBM exhibits highly sensitive accuracy curves, with its task accuracy approaching 100% under full correct intervention and dropping to nearly 0% under full incorrect intervention. However, its initial performance is relatively weak (around 60% on CUB) compared to other models that start above 65% like CEM what exhibits a significantly higher initial performance, achieving 66.36% on CUB and 76.23% on AwA2. However, during correct intervention on AwA2, the CEM improvement is marginal, with the final class accuracy reaching only 80.37% (a gain of about 4%), even when 100% of the concepts are corrected. Besides, when incorrect intervention rate is 100%, the task accuracy only decreases from 76% to 55.60% on AwA2. This indicates that while vanilla CBM offers high interpretability but weak performance, and CEM offers strong performance but poor interpretability.

In contrast, our proposed LDCBM shows superior performance and a better balance. On both datasets, its initial task accuracy is improved by approximately 5% compared to vanilla CBM, while the performance curve remains highly sensitive to concepts. Interestingly, the hybrid model CEM+LDCBM shows beneficial improvements. Its initial performance is boosted by approximately 4% compared to LDCBM alone. Furthermore, the curve’s sensitivity to intervention is enhanced, with the overall range of accuracy change increasing by about 20%, making the model more interpretable than the standard CEM. This indicates that the design of LDCBM effectively helps capture independent concept information and better learn the correspondence between visual patterns and their ground-truth concepts, resulting in a more interpretable and robust hybrid model.

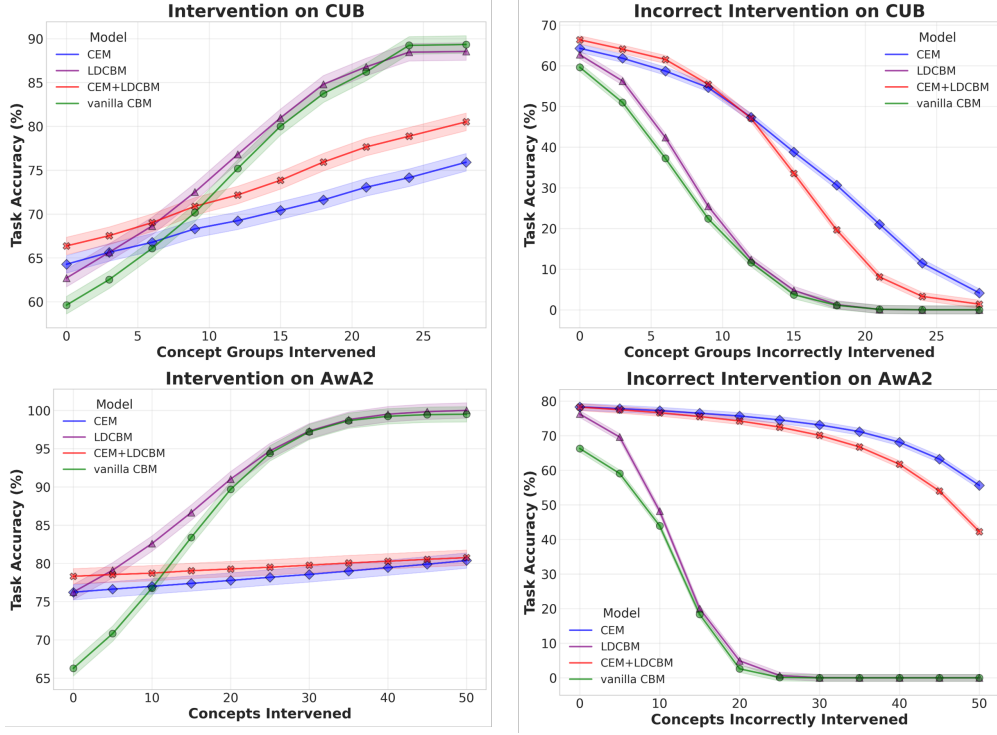


Figure 3: Intervention result of performing correct and incorrect randomly concept interventions in fine-grained and coarse-grained datasets(CUB and AwA2) respectively by four models. Following [4], intervention in CUB, we set groups of related concepts together.

## 5 Conclusion and limitation

In this paper, aims to address and block the CBMs’ gap on input-to-concept data bias and simple the complicated process than other methods. We propose LDCBM, the lightweight and automatic method to recognize the meaningful visual patterns without any region annotation and the image patching. Specifically, our method can automatically find the better alignment between concept ground-truth and coarse and fine grained, we introduce the filter grouping loss to separate different meaningful areas and use the joint concept supervising the grouped filter and achieve the recognized and unique semantic area and concept ground-truth alignment, hence, it is able to find the more interpretable and better performance. Experiments have demonstrated the effectiveness of our method, Our model not only make input-to-concept easier to follow and responsible, but also conducts an in-depth analysis on finding the better interpretation-performance trade-off, towards reducing the potential risks of CBMs in existing black-box and more responsible furture.

## References

- [1] Cynthia Rudin, Chaofan Chen, Zhi Chen, Haiyang Huang, Lesia Semenova, and Chudi Zhong, “Interpretable Machine Learning: Fundamental Principles and 10 Grand Challenges,” July 2021.
- [2] Jake Snell, Kevin Swersky, and Richard S. Zemel, “Prototypical Networks for Few-shot Learning,” June 2017.
- [3] Harrish Thasarathan, Julian Forsyth, Thomas Fel, Matthew Kowal, and Konstantinos Derpanis, “Universal Sparse Autoencoders: Interpretable Cross-Model Concept Alignment,” Feb. 2025.
- [4] Pang Wei Koh, Thao Nguyen, Yew Siang Tang, Stephen Mussmann, Emma Pierson, Been Kim, and Percy Liang, “Concept Bottleneck Models,” Dec. 2020.
- [5] Yue Yang, Artemis Panagopoulou, Shenghao Zhou, Daniel Jin, Chris Callison-Burch, and Mark Yatskar, “Language in a Bottle: Language Model Guided Concept Bottlenecks for Interpretable Image Classification,” Apr. 2023.

- [6] Mateo Espinosa Zarlenga, Pietro Barbiero, Gabriele Ciravegna, Giuseppe Marra, Francesco Giannini, Michelangelo Diligenti, Zohreh Shams, Frederic Precioso, Stefano Melacci, Adrian Weller, Pietro Lio, and Mateja Jamnik, “Concept Embedding Models: Beyond the Accuracy-Explainability Trade-Off,” Dec. 2022.
- [7] Xinyue Xu, Yi Qin, Lu Mi, Hao Wang, and Xiaomeng Li, “Energy-Based Concept Bottleneck Models: Unifying Prediction, Concept Intervention, and Probabilistic Interpretations,” Dec. 2024.
- [8] Eunji Kim, Dahuin Jung, Sangha Park, Siwon Kim, and Sungroh Yoon, “Probabilistic Concept Bottleneck Models,” June 2023.
- [9] Chenming Shang, Shiji Zhou, Hengyuan Zhang, Xinzhe Ni, Yujiu Yang, and Yuwang Wang, “Incremental Residual Concept Bottleneck Models,” in *Proceedings of the IEEE/CVF Conference on Computer Vision and Pattern Recognition*, 2024, pp. 11030–11040.
- [10] Divyansh Srivastava, Ge Yan, and Tsui-Wei Weng, “VLG-CBM: Training Concept Bottleneck Models with Vision-Language Guidance,” .
- [11] Ivaxi Sheth and Samira Ebrahimi Kahou, “Auxiliary Losses for Learning Generalizable Concept-based Models,” Nov. 2023.
- [12] Max Ruiz Luyten, “A Theoretical design of Concept Sets: Improving the predictability of concept bottleneck models,” .
- [13] Konstantinos P Panousis, Dino Ienco, and Diego Marcos, “Coarse-to-Fine Concept Bottleneck Models,” .
- [14] Qihan Huang, Jie Song, Jingwen Hu, Haofei Zhang, Yong Wang, and Mingli Song, “On the Concept Trustworthiness in Concept Bottleneck Models,” Mar. 2024.
- [15] Rui Zhang, Xingbo Du, Junchi Yan, and Shihua Zhang, “The Decoupling Concept Bottleneck Model,” *IEEE Transactions on Pattern Analysis and Machine Intelligence*, vol. 47, no. 2, pp. 1250–1265, Feb. 2025.
- [16] Yan Xie, Zequn Zeng, Hao Zhang, Yucheng Ding, Yi Wang, Zhengjue Wang, Bo Chen, and Hongwei Liu, “Discovering Fine-Grained Visual-Concept Relations by Disentangled Optimal Transport Concept Bottleneck Models,” May 2025.
- [17] Andong Tan, Fengtao Zhou, and Hao Chen, “Explain via Any Concept: Concept Bottleneck Model with Open Vocabulary Concepts,” in *Computer Vision – ECCV 2024*, Aleš Leonardis, Elisa Ricci, Stefan Roth, Olga Russakovsky, Torsten Sattler, and Gü̈l Varol, Eds., Cham, 2025, pp. 123–138, Springer Nature Switzerland.
- [18] Wen Shen, Zhihua Wei, Shikun Huang, Binbin Zhang, Jiaqi Fan, Ping Zhao, and Quanshi Zhang, “Interpretable Compositional Convolutional Neural Networks,” July 2021.
- [19] Samarth Mishra, Pengkai Zhu, and Venkatesh Saligrama, “Interpretable Compositional Representations for Robust Few-Shot Generalization,” *IEEE Transactions on Pattern Analysis and Machine Intelligence*, vol. 46, no. 3, pp. 1496–1512, Mar. 2024.
- [20] Rui Chen, Haifeng Xia, Siyu Xia, Ming Shao, and Zhengming Ding, “IPNet: Interpretable Prototype Network for Multi-Source Domain Adaptation,” in *ICASSP 2025 - 2025 IEEE International Conference on Acoustics, Speech and Signal Processing (ICASSP)*, Apr. 2025, pp. 1–5.
- [21] Anni Yu and Yu-Bin Yang, “Prototypical Part Transformer for Interpretable Image Recognition,” in *ICASSP 2025 - 2025 IEEE International Conference on Acoustics, Speech and Signal Processing (ICASSP)*, Apr. 2025, pp. 1–5.
- [22] Sania Sinha, Tanawan Premriri, and Parisa Kordjamshidi, “A Survey on Compositional Learning of AI Models: Theoretical and Experimental Practices,” Nov. 2024.
- [23] Nuaman Asbeh and Boaz Lerner, “Learning Latent Variable Models by Pairwise Cluster Comparison,” in *Proceedings of the Asian Conference on Machine Learning*. Nov. 2012, pp. 33–48, PMLR.
- [24] Jiguang Wang, “Pearson Correlation Coefficient,” in *Encyclopedia of Systems Biology*, pp. 1671–1671. Springer, New York, NY, 2013.
- [25] Zhangzhang Si and Song-Chun Zhu, “Learning AND-OR Templates for Object Recognition and Detection,” *IEEE Transactions on Pattern Analysis and Machine Intelligence*, vol. 35, no. 9, pp. 2189–2205, Sept. 2013.
- [26] Xiangteng He and Yuxin Peng, “Fine-grained Visual-textual Representation Learning,” *IEEE Transactions on Circuits and Systems for Video Technology*, vol. 30, no. 2, pp. 520–531, Feb. 2020.
- [27] Ziwei Liu, Ping Luo, Xiaogang Wang, and Xiaoou Tang, “Deep Learning Face Attributes in the Wild,” Sept. 2015.
- [28] Yongqin Xian, Christoph H. Lampert, Bernt Schiele, and Zeynep Akata, “Zero-Shot Learning – A Comprehensive Evaluation of the Good, the Bad and the Ugly,” Sept. 2020.